PNNL-24698

Pacific Northwest
NATIONAL LABORATORY
Proudly Operated by Battelle Since 1965

Geostatistical Realizations of WMA-C Lithofacies

September 2015

Z Hou
Y Bott
CJ Murray

U.S. DEPARTMENT OF ENERGY

Prepared for the U.S. Department of Energy
under Contract DE-AC05-76RL01830

PACIFIC NORTHWEST NATIONAL LABORATORY
operated by
BATTELLE
for the
UNITED STATES DEPARTMENT OF ENERGY
under Contract DE-AC05-76RL01830

Printed in the United States of America

Available to DOE and DOE contractors from the
Office of Scientific and Technical Information,
P.O. Box 62, Oak Ridge, TN 37831-0062;
ph: (865) 576-8401
fax: (865) 576-5728
email: reports@adonis.osti.gov

Available to the public from the National Technical Information Service
5301 Shawnee Rd., Alexandria, VA 22312
ph: (800) 553-NTIS (6847)
email: orders@ntis.gov <http://www.ntis.gov/about/form.aspx>
Online ordering: http://www.ntis.gov


This document was printed on recycled paper.
(8/2010)

PNNL-24698

Geostatistical Realizations of WMA-C Lithofacies

Z Hou Y Bott
CJ Murray

September 2015

Prepared for
the U.S. Department of Energy
under Contract DE-AC05-76RL01830

Pacific Northwest National Laboratory
Richland, Washington 99352

Abstract

This report documents the development of a set of detailed facies-based geologic conceptual models of the subsurface beneath the Waste Management Area (WMA) C, which is located in the 200 East Area of the Central Plateau at Hanford Site in southeast Washington. WMA C is one of 12 tank farms within 7 WMAs (A-AX, B-BX-BY, C, S-SX, T, TX-TY, and U) containing 149 SSTs and ancillary equipment built at the Hanford Site from 1943 to 1964.

The conceptual models developed under this effort will provide the basis for some supporting alternative conceptual and numerical models and some selected sensitivity cases that are being used to support a long-term performance assessment (e.g. human health and environmental impacts analysis) of WMA C when it is eventually closed. This performance assessment is being used by the U.S. Department of Energy, Office of River Protection (DOE-ORP) to evaluate closure of WMA C under Federal requirements and forthcoming State-approved closure plans and permits in accordance with the Hanford Federal Facility Agreement and Consent Order (HFFACO) (Ecology, EPA et al. 1989), Action Plan, Appendix I.

Lithofacies (lithologies having similar physical and chemical properties) are identified by multivariate analysis of spectral gamma radiation (SGR) data for natural potassium, uranium, and thorium (KUT). KUT data can be used to identify sediment types with different geological and hydrological properties, while geostatistical analysis yields continuity in lithofacies for further modeling purposes. At the WMA C, vertical continuity in lithofacies can be estimated from wellbore data. The well data is insufficient though to identify horizontal continuity, and an assumption that lithofacies are 10 times more continuous horizontally than vertically is adopted. Alternative conceptual models are made possible by varying this assumption. Multiple realizations of lithofacies distribution are then generated using indicator simulation methods. Each realization honors the borehole data, and reproduces the spatial model of lithofacies continuity between boreholes. All the realizations incorporate heterogeneity of lithofacies, rather than treating stratigraphic units as homogeneous layers.

Summary

One critical aspect of the long-term performance assessments for closed facilities containing radiological and hazardous chemical wastes is the evaluation of contaminant flow and transport from source areas via the groundwater pathway through the use of numerical simulations with the associated uncertainties quantified. Information on the spatial distribution and heterogeneity of the subsurface properties that affect flow and transport is often very limited. However, understanding of the sedimentary geology and particularly the spatial distribution of lithofacies can be used to constrain estimates on the spatial distribution and heterogeneity of subsurface sediments.

This report documents the development of a set of detailed facies-based geologic conceptual models of the subsurface beneath the Waste Management Area (WMA) C, which is located in the 200 East Area of the Central Plateau at Hanford Site in southeast Washington. WMA C is one of 12 tank farms within 7 WMAs (A-AX, B-BX-BY, C, S-SX, T, TX-TY, and U) containing 149 SSTs and ancillary equipment built at the Hanford Site from 1943 to 1964.

The conceptual models developed under this effort will provide the basis for some supporting alternative conceptual and numerical models and some selected sensitivity cases that are being used to support a long-term performance assessment (e.g. human health and environmental impacts analysis) of WMA C when it is eventually closed. This performance assessment is being used by the U.S. Department of Energy, Office of River Protection (DOE-ORP) to evaluate closure of WMA C under Federal requirements and forthcoming State-approved closure plans and permits in accordance with the Hanford Federal Facility Agreement and Consent Order (HFFACO) (Ecology, EPA et al. 1989), Action Plan, Appendix I.

Currently, existing conceptual models of the geologic framework being used for the WMA-C PA are represented by the large-scale hydrogeologic units identified at the site. The intent of this effort is to develop alternative conceptual models that attempt to reproduce the detailed heterogeneity of sediments within the major hydrogeologic units found beneath the WMA C. This development work will be based on geostatistical analysis of available geophysical and borehole log data and information at the WMA C. The initial set of multiple realizations of the subsurface conditions developed from this effort will provide the basis for a quantitative modeling analysis being performed at PNNL under separate funding using the ASCEM (Advanced Simulation Capability for Environmental Management) Toolset (Freshley, Hubbard et al. 2012). In the coming year, this ASCEM modeling demonstration effort will be used to perform an initial evaluation of the impacts of heterogeneities on past leaks and tank residuals at the WMA C.

Borehole data and information are the cornerstone of subsurface characterization, monitoring, and performance assessment programs. Spectral gamma radiation (SGR) logging data were collected in a number of wells and boreholes in the vicinity of the WMA C. Specific data on natural potassium, uranium, and thorium that were collected as part of the SGR logging data were used in multivariate clustering analysis including k-means and expectation-maximization (EM) clustering. Geostatistical indicator variograms were modeled for the identified lithofacies distributions. The indictor variogram models for lithofacies were the basis for a sequential indicator simulation approach to generate realizations of lithofacies fields over the modeling domain. Sequential indicator simulation (SISIM) was applied to generate multiple realizations of lithofacies distributions by assigning values to grid nodes along random paths through all of the grid nodes, conditioning on nearby data including values at

previously simulated grid nodes. The sequential indicator simulation approach honors spatial heterogeneity within the major geologic units and captures spatial continuity and correlation patterns in the lithofacies.

Acknowledgments

This study is performed under Washington River Protection Solutions (WRPS) MOA Number TOC-MOA-PNNL-0002, in accordance with Prime Contract Number DE-AC27-08RV14800. The J3 Identifier for this work is 93.

Acronyms and Abbreviations

Advanced Simulation Capability for Environmental Management	ASCEM
Bayesian Information Criterion	BIC
Expectation Maximization	EM
Hanford Federal Facility Agreement and Consent Order	HFFACO
Office of River Protection	ORP
Pacific Northwest National Laboratory	PNNL
Performance Assessment	PA
Potassium/uranium/thorium	KUT
Sequential indicator simulation	SISIM
Spectral Gamma Radiation	SGR
Subsurface Transport Over Multiple Phases	STOMP
Waste Management Area	WMA

Contents

Figures

Tables

1.0 Introduction

This report documents the development of a set of detailed facies-based geologic conceptual models of the subsurface beneath the Waste Management Area (WMA) C, which is located in the 200 East Area of the Central Plateau at Hanford Site in southeast Washington. WMA C is one of 12 tank farms within seven WMAs (A-AX, B-BX-BY, C, S-SX, T, TX-TY, and U) containing 149 SSTs and ancillary equipment built at the Hanford Site from 1943 to 1964.

The conceptual models developed under this effort will provide the basis for implementation of some supporting alternative conceptual and numerical models and evaluation of some selected sensitivity cases that are being used to support a long-term performance assessment (e.g. human health and environmental impacts analysis) of WMA C when it is eventually closed. This performance assessment is being used by the U.S. Department of Energy, Office of River Protection (DOE-ORP) to evaluate closure of WMA C under Federal requirements and forthcoming State-approved closure plans and permits in accordance with the Hanford Federal Facility Agreement and Consent Order (HFFACO) (Ecology, EPA et al. 1989), Action Plan, Appendix I. The scope of the analysis evaluates the human health and environmental impacts from radioactive and hazardous chemical constituents contained in both residual wastes left in the tanks and ancillary equipment at closure as well as the contaminated soils impacted by past leaks and releases of wastes from WMA C during its historical operations.

One critical component of the PA effort is the evaluation of contaminant flow and transport from source areas through a 75 to 80 m thick sequence of vadose zone sediments, and to the unconfined aquifer at WMA C via numerical simulations with the associated uncertainties quantified. However, information on the spatial distribution and heterogeneity of the subsurface properties that control flow and transport is often very limited. Instead of producing realizations of subsurface properties/parameters that directly incorporate uncertainty, a better way to incorporate spatial heterogeneity and variability is to understand the effect of sedimentary geology, particularly lithofacies, on the spatial distribution of flow/transport parameters. The spatial distribution of lithofacies can be derived from borehole data and used to constrain estimates on the spatial distribution and heterogeneity of key subsurface flow and transport properties (Deutsch 2002, Scheibe, Fang et al. 2006, Yabusaki, Fang et al. 2011, Freedman, Chen et al. 2014).

Borehole data are the cornerstone of subsurface characterization, monitoring, and performance assessment programs. Lithofacies classification for borehole geology has, in general, been based on many different log responses and characteristics (Kumar and Kear 2003, Maiti, Tiwari et al. 2007). Borehole image data are a proven, valuable resource for geological evaluation. Another useful device is the borehole spectroscopy tool, which generates the broad elemental composition of the rock and its quantitative geochemical lithology (Hertzog, Colson et al. 1989, Galford, Quirein et al. 2009). The two outputs complement each other well to support detailed interpretations of geologic conditions.

Various clustering techniques can be used for borehole data classification. Among the various algorithms, k-means clustering is a method of vector quantization, originally from signal processing, which is popular for cluster analysis in data mining. K-means clustering aims to partition n observations into k clusters in which each observation belongs to the cluster with the nearest mean, serving as a prototype of the cluster. Probability models have successfully formed a basis for cluster analysis. According to recent studies, clustering procedures based on probability models are increasingly favorable

over heuristic methods (Fraley and Raftery 2002, Lau and Green 2007), where each cluster may correspond to a particular characteristic such as orientation, volume, or shape. A maximum likelihood criterion of Gaussian clustering was developed to allow characteristics to vary for clusters, preserving the shapes of the clusters while varying orientation and volumes (Banfield and Raftery 1993).

The finalized clusters can be treated as lithofacies, which then can be used for geostatistical indicator analysis including variogram modeling and sequential indictor simulation of lithofacies over the modeling domain. The indicator approach is particularly useful when attributes vary over orders of magnitude. The indicator approach allows the representation of facies occurrences as discrete entities, while the in-facies distribution with lower variance such as permeability can be better represented with geostatistical methods for continuous variables (Rubin and Journel 1991, Bierkens 1996, Goovaerts 1997, Ritzi 2000, Deutsch 2002, Deutsch 2006). Moreover, lithological data are typically more abundant than permeability data. When permeability data may be lacking, lithological data can be used with the indicator approach to represent at least the coarser aspects of heterogeneity.

Indictor variogram models for lithofacies can be incorporated in an indicator simulation approach to generate realizations of lithofacies fields over the numerical modeling domain. Sequential indicator simulation (SISIM) is one of the most popular methods (Deutsch and Journel 1998). SISIM transforms the categorical lithology data into a vector of indicator data, and defines a random path through each grid node only once. At each grid node, the conditional probability of occurrence of each lithofacies is established using simple or ordinary kriging with the conditioning information of nearby original indicator data and previously simulated indicator values, upon which a cumulative distribution function is defined by adding the corresponding probabilities of occurrences of all lithofacies categories. With a randomly drawn probability value, a simulated value is then assigned based on the cumulative distribution function (Goovaerts 1997, Deutsch and Journel 1998). In modeling applications such as being done for the WMA C PA effort, given the lithofacies realizations, the permeability fields can be generated by drawing from the in-facies distribution of permeability, and used by the numerical modeling team.

2.0 Site and Data Description

The Waste Management Area C is one of seven WMAs (A-AX, B-BX-BY, C, S-SX, T, TX-TY, and U), and is located in the Hanford 200 East Area, see Figure 1. The tank farm site was constructed in 1943-1944, and operated from 1946 through mid-1980s for storing and transferring waste. Over the long operational history, the WMA C received waste generated by essentially all major chemical processing operations at the Hanford site, with a total past releases of about 149,600 Gal (RPP-RPT-42294, Rev. 1 *Hanford Waste Management Area C Soil Contamination Inventory Estimates*, and the residual wastes containing inventories of ^{99}Tc, uranium, and chromium. The vadose zone above the unconfined aquifer and below backfill has been considered to consist of three major hydrostratigraphic units: H1 gravelly sand, H2 sand, and H3 gravelly sand (RPP-RPT-56356, *Development of Alternative Digital Geologic Models of Waste Management Area C).*

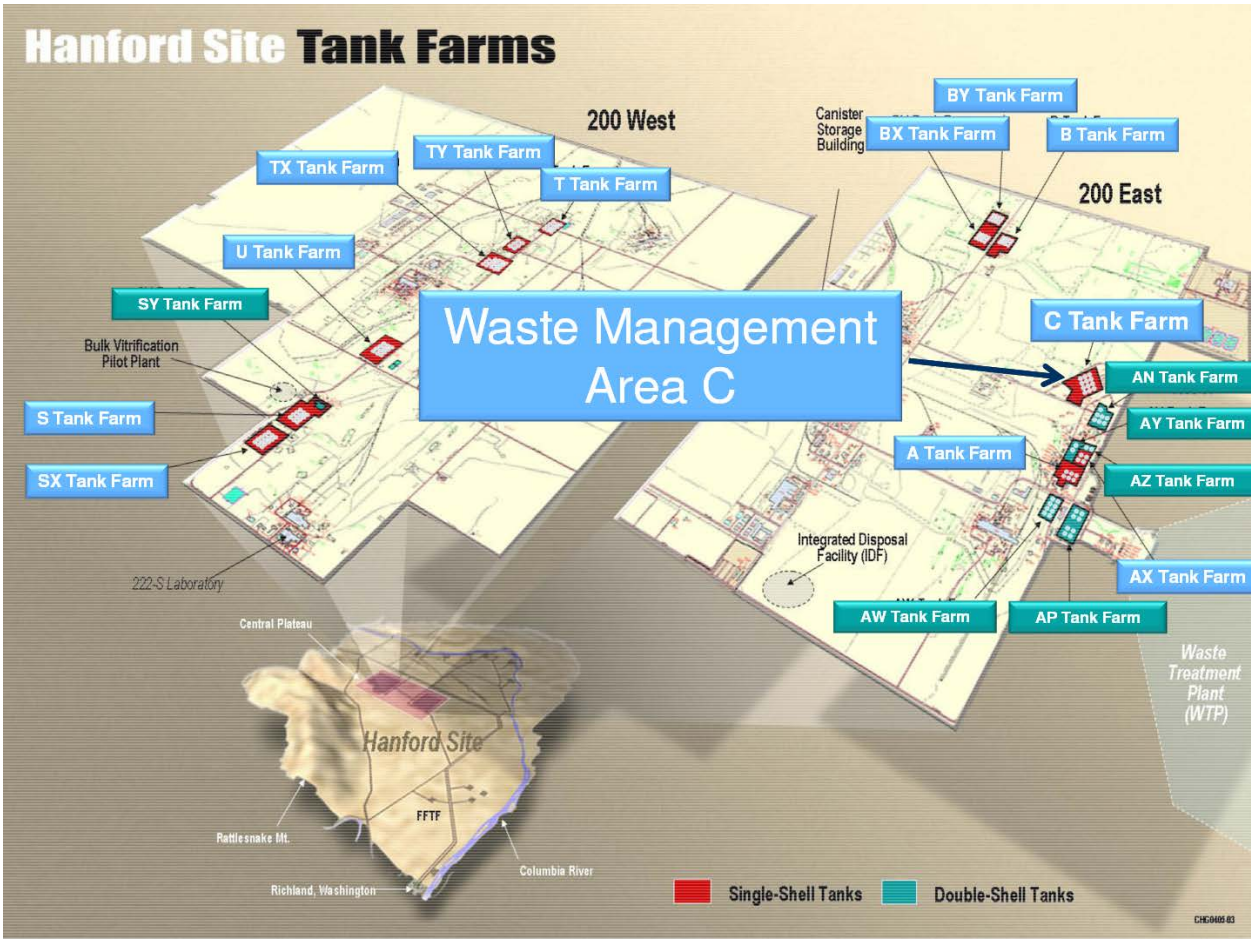

Figure 1. The locations of Waste Management Area C (WMC C) (from Bergeron and Aly, 2014)

Numerical models were developed to estimate the contaminant concentrations within water, air, or soil as a function of time. Three-dimensional flow and transport models have been developed based on the Subsurface Transport Over Multiple Phases (STOMP) code developed by Pacific Northwest National Laboratory (White and Oostrom 2006), and are being used to evaluate the impact of radiological and hazardous chemical constituents to the environment along the groundwater pathway from the proposed closure of the WMA C tanks. The flow and transport parameters (e.g., permeability) that are needed by

the numerical models are inferred from well log data and information collected from 25 boreholes in the study area (Figure 2).

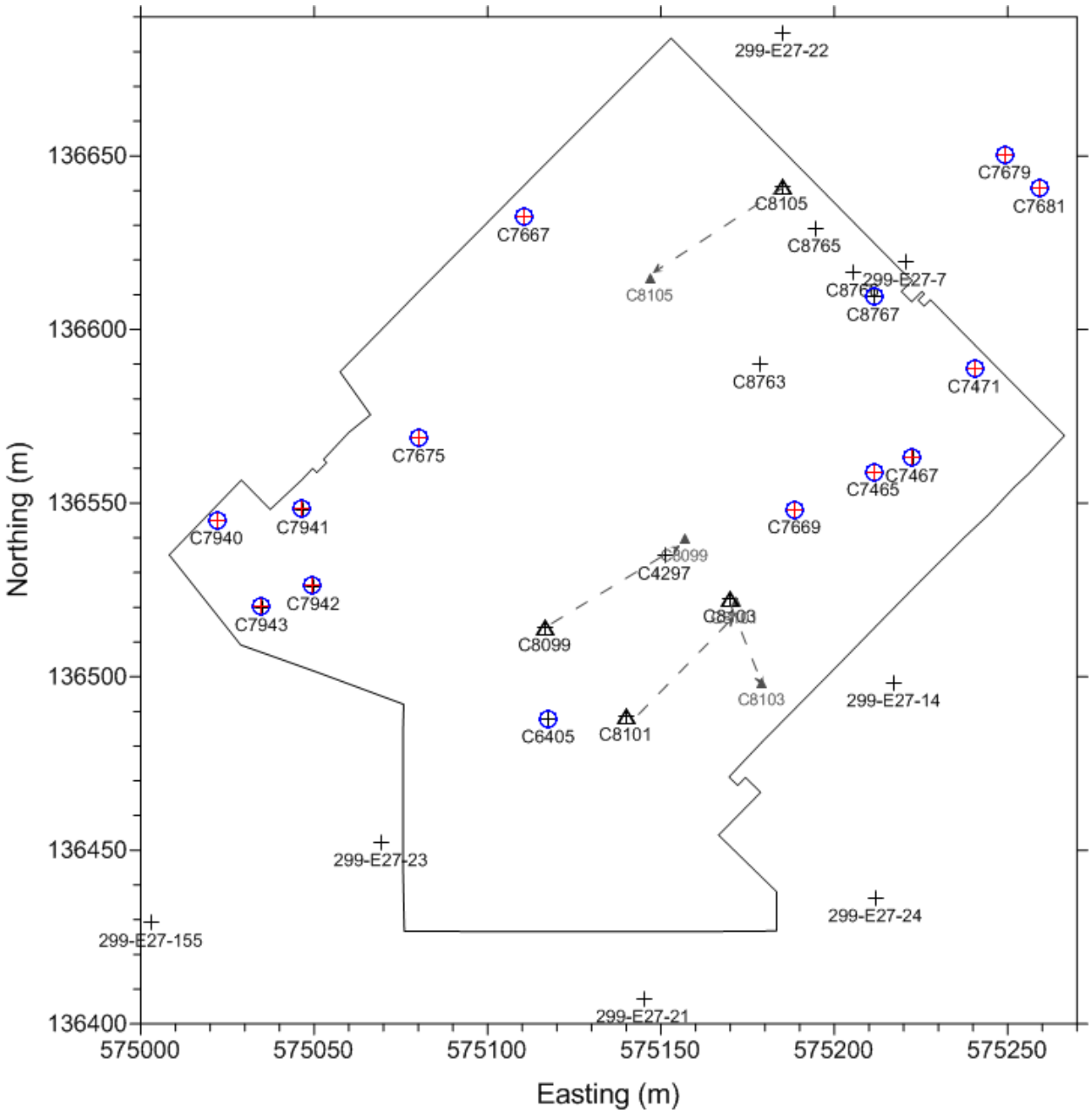

Figure 2. Locations of 25 WMA-C Wells with spectral gamma radiation data (black crosses) with depths greater than 50 m, 14 wells with moisture data (blue circles), and four angled direct push wells (black triangles). The 12 vertical direct push wells chosen for analysis are marked with red crosses.

Selected WMA-C wells and boreholes evaluated in this analysis are shown on Figure 2 and are listed in Table 1. The wells and boreholes considered include seven groundwater monitoring wells, one deep characterization borehole, seventeen vertical direct push boreholes, and four angled direct push boreholes. Volumetric water content data are available for the fourteen direct push boreholes. The sampling intervals are about 0.5 ft for the natural potassium, uranium, and thorium (KUT) data collected as a part

of the spectral gamma radiation (SGR) logging data and 0.25 ft for volumetric water content developed from neutron moisture logging. The measurements are dated from August 2003 to May 2013. As we are interested in wells with measurements more representative over various stratigraphic units above the water table, such as H1, H2, H2-Coarse and even H2-Silt, only wells with KUT and moisture content measurements over 50 m, except for two angled direct push boreholes, were chosen to be included in the initial data exploratory analysis.

Table 1. Summary of WMA-C Wells with KUT and Volumetric Water Content Data over 50 m and Angled Direct Push Boreholes

Well Name	Easting (m)	Northing (m)	Length of KUT (m)	Length of Moisture Content (m)	Well Type	Log Date
299-E27-7	575220.59	136619.40	79.86		Groundwater Well	Jan. 2008
299-E27-14	575217.34	136498.24	82.30		Groundwater Well	Mar. 2007
299-E27-21	575145.03	136407.21	96.32		Groundwater Well	Jul. 2003
299-E27-22	575185.10	136685.33	80.60		Groundwater Well	Sep. 2003
299-E27-23	575069.46	136452.23	97.23		Groundwater Well	Aug. 2003
299-E27-24	575212.03	136436.28	96.62		Groundwater Well	May 2010
299-E27-155	575003.11	136429.08	102.70		Groundwater Well	Oct. 2007
C4297	575151.18	136534.78	59.32		Deep Characterization	Mar. 2004
C6405	575117.70	136487.80	72.92	73.15	Direct Push	Mar. 2009
C7465	575211.40	136559.00	61.72	61.49	Direct Push	Jul. 2009
C7467	575222.63	136563.00	52.73	52.88	Direct Push	Jul. 2009
C7471	575240.60	136588.60	67.82	67.59	Direct Push	Dec. 2009
C7667	575110.60	136632.30	67.67	67.59	Direct Push	Dec. 2009
C7669	575188.70	136548.10	67.67	67.59	Direct Push	Dec. 2009
C7675	575080.40	136568.70	67.21	67.13	Direct Push	Jun. 2010
C7679	575249.30	136650.30	53.56	54.25	Direct Push	Jun. 2010
C7681	575259.40	136640.50	66.98	67.06	Direct Push	Jun. 2010
C7940	575022.00	136545.00	61.87	61.57	Direct Push	Oct. 2010
C7941	575047.00	136548.00	61.57	61.57	Direct Push	Oct. 2010
C7942	575050.00	136526.00	61.87	61.57	Direct Push	Oct. 2010
C7943	575035.00	136520.00	61.80	61.65	Direct Push	Oct. 2010
C8763	575178.60	136589.94	65.47		Direct Push	Apr. 2013
C8765	575194.45	136629.20	62.49		Direct Push	May 2013
C8766	575205.48	136616.35	62.49		Direct Push	May 2013
C8767	575211.47	136609.30	62.48	63.70	Direct Push	May 2013
C8099	575116.69	136514.24	60.89		Angled Direct Push	-
C8101	575140.04	136488.43	53.70		Angled Direct Push	-
C8103	575170.06	136522.43	45.09		Angled Direct Push	-
C8105	575184.94	136641.24	22.58		Angled Direct Push	-

3.0 Identification of Lithofacies

Lithofacies are lithologies with similar physical and chemical properties. At the wells described previously, spectral gamma ray (SGR) logging data for KUT are available and can be used to identify sediment types with different geological and hydrological properties. Summary statistics were first generated for the KUT data, which shows significantly different distributions among different stratigraphic units (Figure 3), especially for natural potassium (Figure 4) and natural thorium.

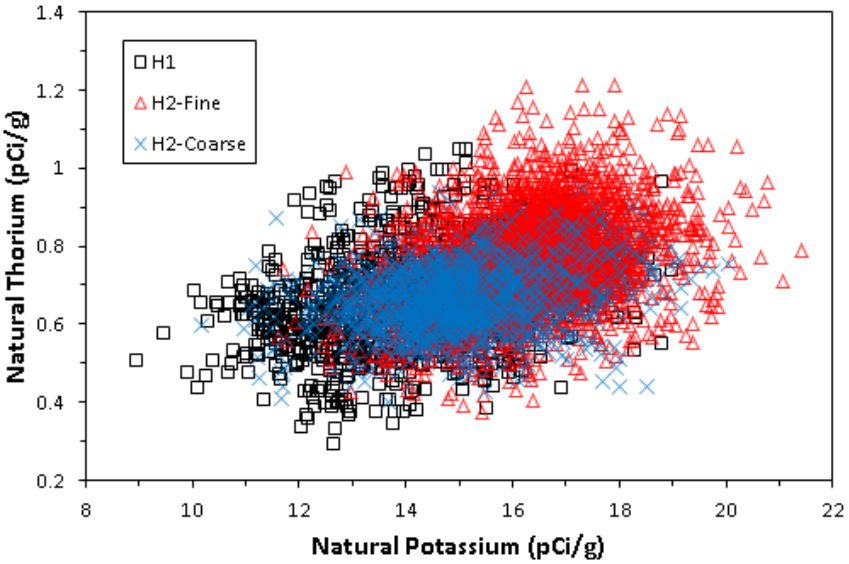

Figure 3. The scatter plot of natural thorium and natural potassium for three stratigraphic units.

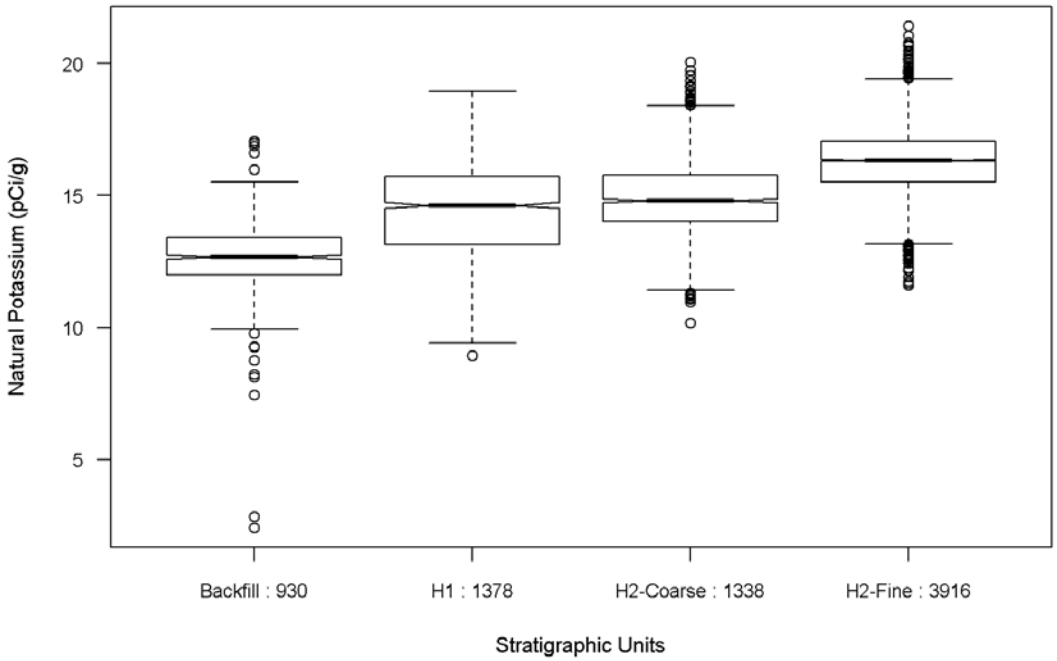

Figure 4. Boxplots of natural potassium in different stratigraphic units.

In previous studies at BC-Cribs (Freshley, Hubbard et al. 2012), these variations were directly related to lithology using ROCSAN data on particle size. Therefore, cluster analysis of KUT data developed from spectral gamma logging can be performed to identify clusters to be treated as lithofacies. The initial approach focused on boreholes over 50 m deep, including groundwater wells (Table 1). Significant deviations were found for KUT data from several of the groundwater wells. Meanwhile, significant bentonite grout was found present adjacent to the casing in the groundwater wells, which affected KUT data. Per communication with colleague M. Connelly, a majority of the KUT data from groundwater wells was questionable. It is also worth noting that some variability was found in the direct push KUT data related to instrument differences in vertical vs. angled boreholes. Therefore only 12 vertical direct push boreholes were included in the following studies, which are marked red in Table 1.

Probability-based clustering was performed using the MCLUST algorithm implemented in R (Fraley and Raftery 2002). EM-clustering assumes a Gaussian mixture model, and the mixture likelihood approach maximizes

$$\prod_{i=1}^{n}\sum_{k=1}^{G}\tau_k f_k(x_i \mid \theta_k), \quad (1)$$

where $\boldsymbol{x} = (x_1, \ldots, x_n)$ represents the data, G is the number of components in the mixture, and τ_k is the probability that an observation belongs to the k^{th} component ($\tau_k \geq 0$; $\sum_{k=1}^{G}\tau_k = 1$). The parameters θ_k consist of a mean vector μ_k and a covariance matrix Σ_k, and the density has the form

$$f_k(x_i \mid \mu_k, \Sigma_k) = (2\pi)^{-p/2}|\Sigma_k|^{-1/2} exp\left\{-\frac{1}{2}(x_i - \mu_k)^T \Sigma_k^{-1}(x_i - \mu_k)\right\}, \quad (2)$$

where the covariance matrix $\Sigma_k = \lambda_k D_k A_k {D_k}^T$, D_k is the orthogonal matrix of eigenvectors that determine the orientation of the principal components of Σ_k, A_k is a diagonal matrix whose elements are proportional to the eigenvalues of Σ_k, and λ_k is a scalar that controls the shape of the density contours and specifies the volume of the corresponding ellipsoid. These parameters enable the flexibility of using different orientations, shapes, and volumes for the classes in the multivariate data space. With adjustments of the parameters λ_k, D_k, and A_k, the resulting classes from EM-clustering are ellipsoidal with orientations, shapes, and volumes varying from class to class. Because of the many options of assigning ensemble members to classes, it is important to adopt a well-accepted criterion to choose from the many models by penalizing the number of classes while honoring the likelihood of a member belonging to its assigned class. The model selection was based on Bayesian Information Criterion (BIC) (Schwarz 1978) that has the form

$$BIC \equiv 2loglik_{\mathcal{M}}(\boldsymbol{x}, \theta_k^*) - m\log(n), \quad (3)$$

where the $loglik_{\mathcal{M}}(\boldsymbol{x}, \theta_k^*)$ is the maximized mixture log-likelihood for the model, m is the number of independent parameters ($\theta_k^*, k = 1, \ldots, m$) to be estimated in the model, and n is the number of observations of the data $\boldsymbol{x} = (x_1, \ldots, x_n)$. The larger the value of BIC is, the stronger the evidence (i.e., the more likely) supporting the selection of the model and the number of clusters.

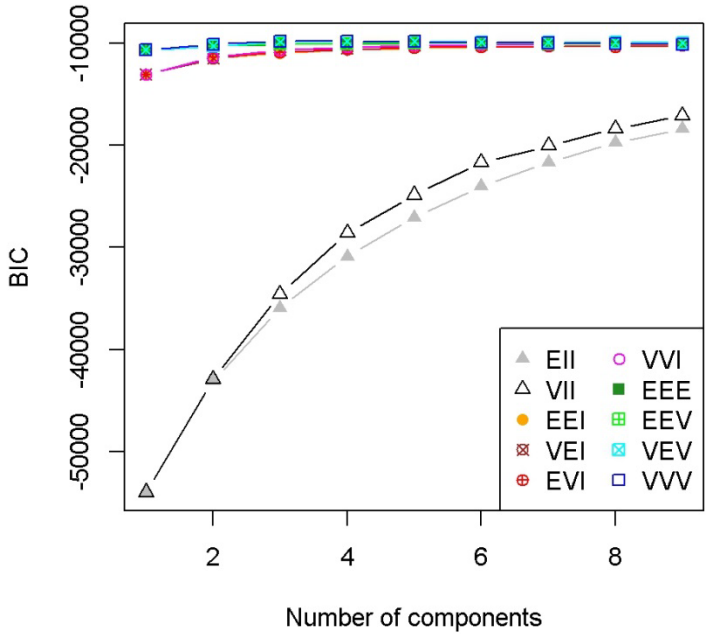

Figure 5. BIC vs. number of Components from Mclust using the KUT Data.

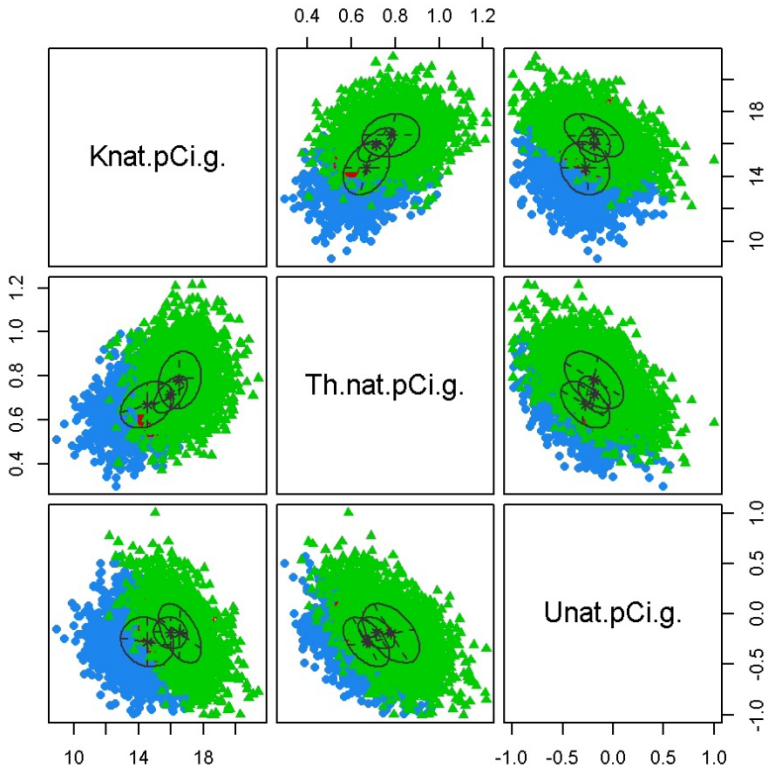

Figure 6. Best classification of three lithofacies from Mclust with the KUT Data.

Given the model selection criterion BIC, the EM-clustering resulted in three clusters (lithofacies) for the available KUT data (Figure 5 and Figure 6). Lithofacies 1 appears to be of intermediate texture and small portion, about 4% of the data. It is low in natural potassium and high but variable in natural thorium. Lithofacies 2 is associated with coarse textured sediments, lower natural potassium and natural

thorium. Lithofacies 3 is more of sandy texture and marked by higher natural potassium and natural thorium (Figure 7).

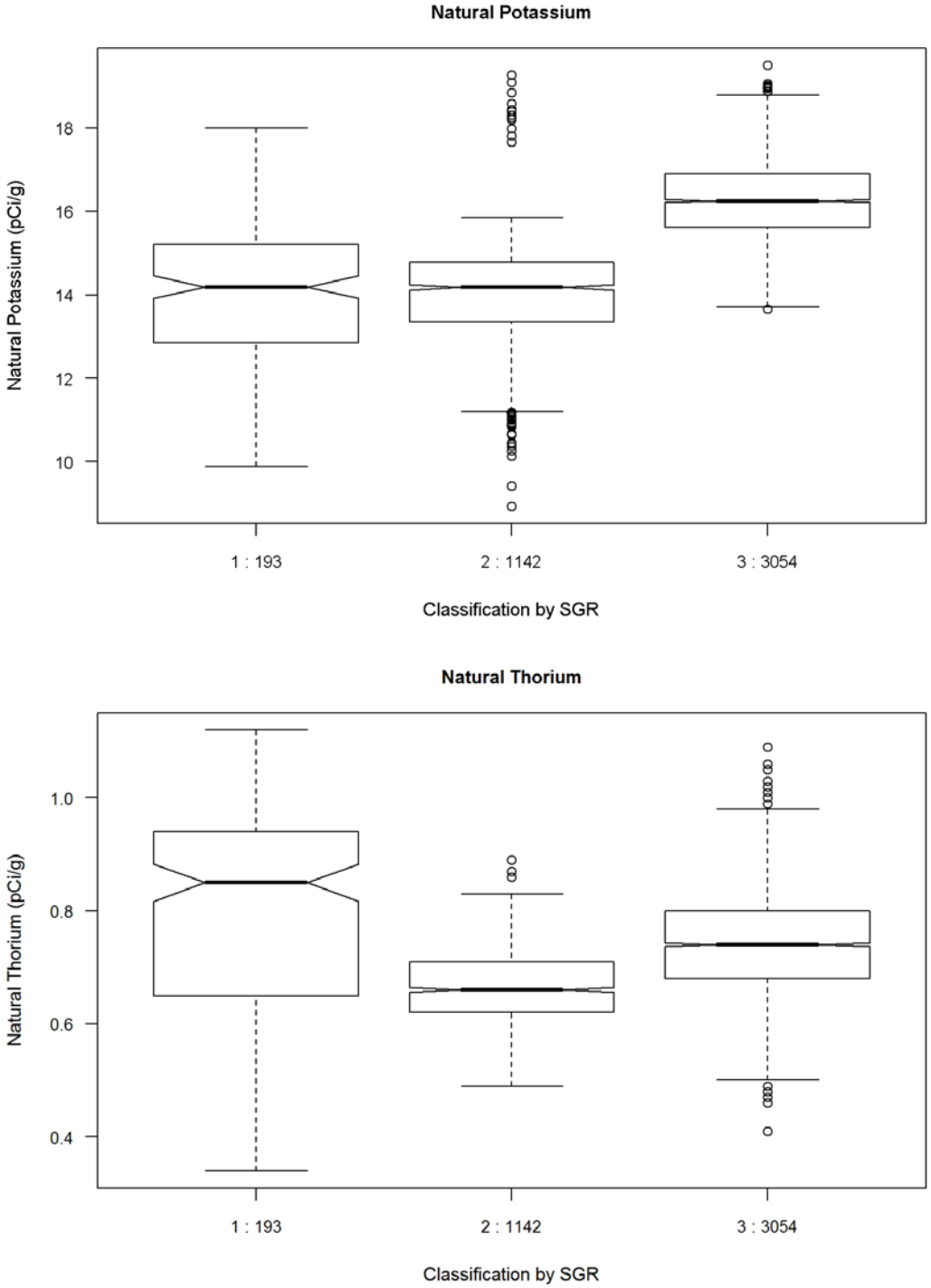

Figure 7. Boxplots of natural potassium and natural thorium for three identified lithofacies using EM-clustering.

Figure 8 displays the vertical distribution of the three identified lithofacies along the direct push boreholes. The lithofacies units are closely associated with stratigraphic units: Lithofacies 3 (red) is identified as sandy lithofacies and is concentrated in the H2 Fine unit; Lithofacies 2 (green) is identified as a gravel rich lithofacies that is concentrated in the H2 Coarse unit; Lithofacies 1 (blue) appears to be of intermediate texture and rare (about 4% of data). Comparatively, the stratigraphic unit H1 appears to be comprised of equal amounts of gravel & sand; H2 Fine is dominated by sandy lithofacies 3; while H2 Coarse is dominated by gravel lithofacies of Lithofacies 2. In general, heterogeneous but correlative distributions of lithofacies can be seen in each stratigraphic unit.

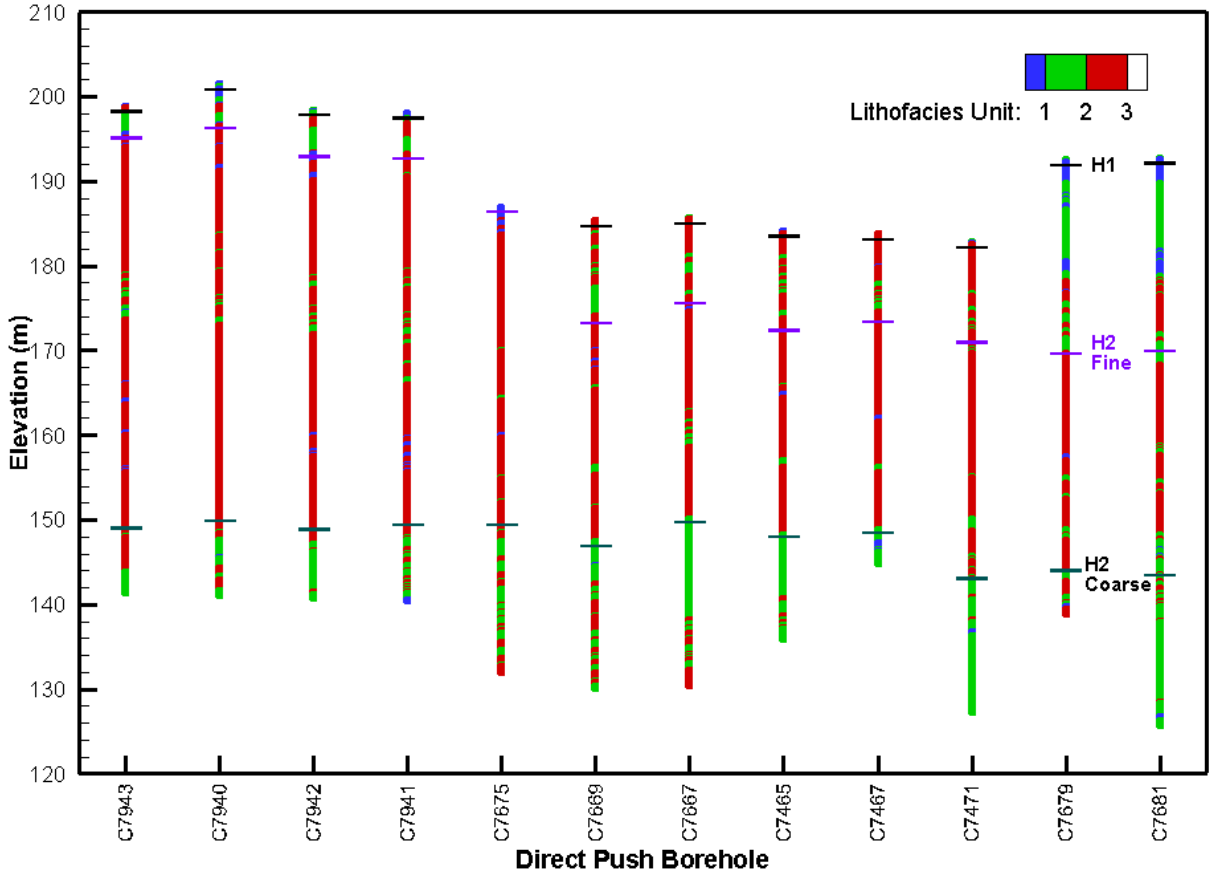

Figure 8. Distribution of the three lithofacies, and the stratigraphic units along the direct push boreholes.

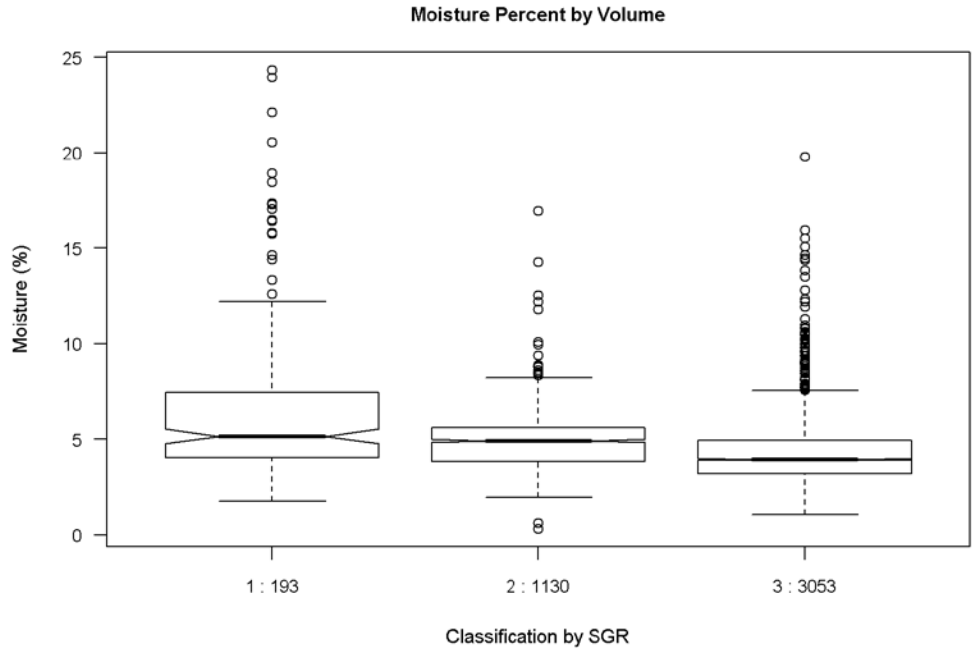

Figure 9. Boxplots of soil moisture for three identified lithofacies using EM-clustering.

One interesting thing to look at is the distribution of soil moisture content corresponding to the lithofacies, especially since both lithofacies 3 and 1 are associated with a tail of higher moisture values. As shown in Figure 9, volumetric moisture did not appear to be strongly associated with potassium/uranium/thorium (KUT) values. The preliminary study suggested that adding moisture to KUT data set did not result in significant improvement in clustering of lithofacies (Figure 10). This is probably because of heterogeneous distribution of artificial recharge, so that the moisture data may be influenced by transport in the vadose zone as well as lithology.

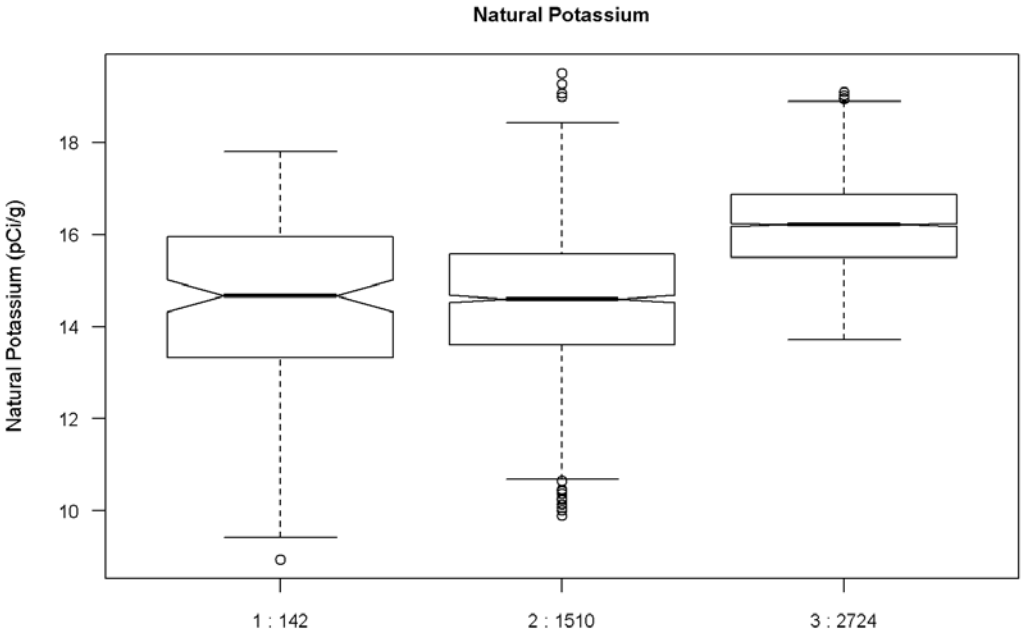

Figure 10. Boxplots of natural potassium for three preliminary lithofacies using EM-clustering with natural potassium, natural thorium and volumetric moisture content.

4.0 Variogram Modeling of Lithofacies

Given the spatial distributions of lithofacies along the boreholes, experimental indicator variograms were well-defined vertically. Various models were evaluated, and nested spherical models were chosen for the three lithofacies (Figure 11). The fitted vertical indicator variogram model parameters for the three lithofacies are listed in Table 2. Because of lack of information about the horizontal ranges, the anisotropy ratio of the horizontal to vertical range is assumed to be 10:1. In future studies, the anisotropy ratio could also be treated as a varying parameter in uncertainty analysis to determine sensitivity of transport to anisotropy ratio.

Table 2. Fitted vertical indicator variogram model parameters for the three lithofacies.

Lithofacies	Nugget	Sill	Vertical Range (m)	Horizontal Range (m)
1	0.2	0.46	1	10
		0.34	15	150
2	0.1	0.37	1	10
		0.53	16	160
3	0.14	0.36	1.2	12
		0.50	22	220

The variograms correspond to the vertical distributions of the three lithofacies well. As shown on Figure 8, lithofacies 1 usually spans less than 20 m along the boreholes, which results in a variogram with most variabilities within 10 m. At first look the models for lithofacies 2 and 3 seem similar. The distributions of the sandy lithofacies 3 are generally longer and more continuous along the boreholes, hence the variogram and its modeled range is longer than the gravelly lithofacies 2.

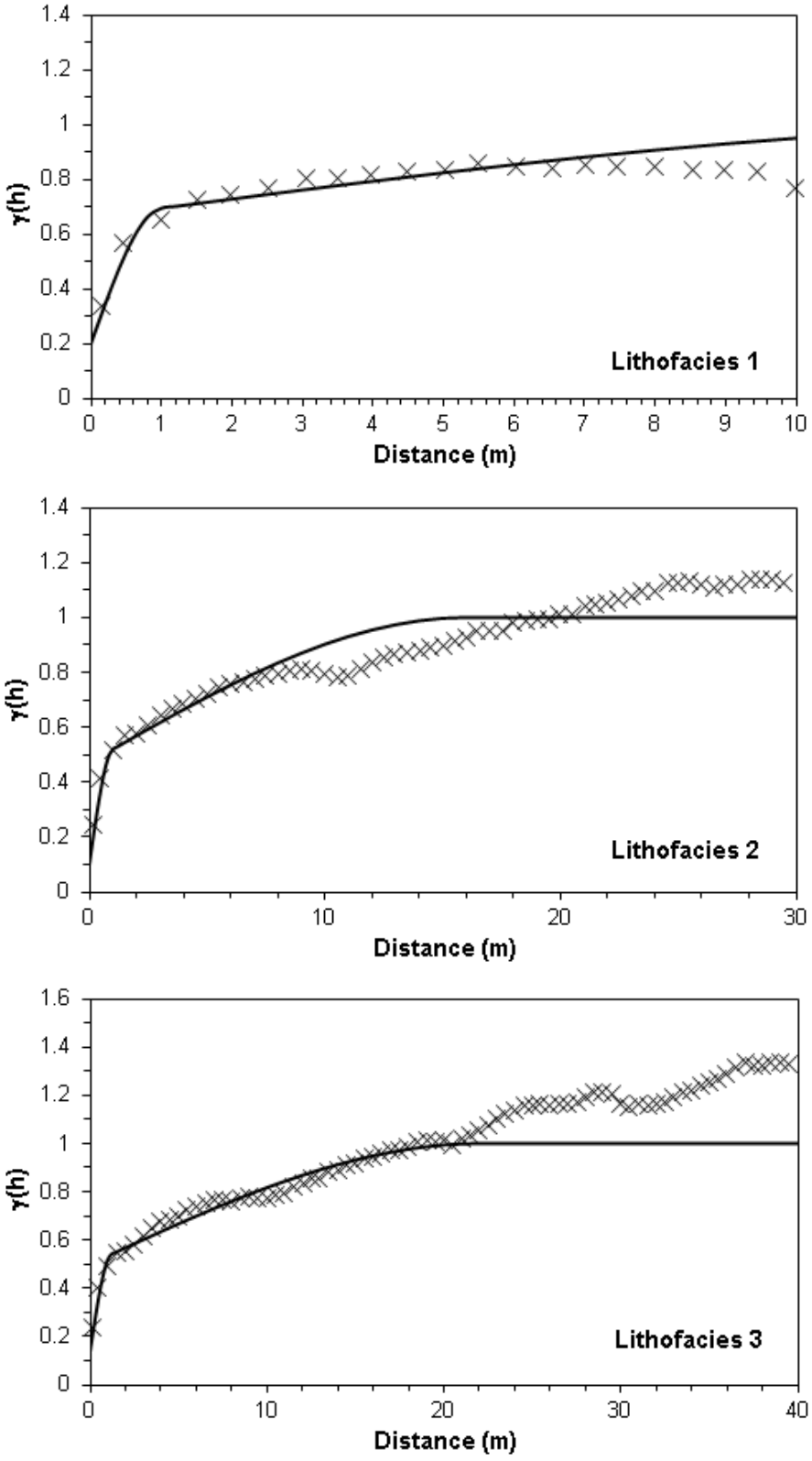

Figure 11. Fitted vertical indicator variograms for three identified lithofacies.

5.0 Simulation of Lithofacies Distribution

Considering the lack of spatial coverage of the direct push boreholes in the WMA-C area, we employed a pseudo-well approach that we also used for the BC-Cribs site study (Freshley, Hubbard et al. 2012). The added pseudo-wells are included in the conditioning data set, and the data were replicated from the closest boreholes at those locations. This approach helps reinforce layering of lithofacies seen in borehole data and still honors spatial heterogeneity in lithofacies.

Based on analysis of gradient of H2 Silt surface, it is assumed that there exists a constant 2.3 degree dip to the northeast, which is due north in rotated coordinates (see Figure 12). This dip is incorporated into the variogram model. The rotated coordinates were defined to align with the northwest to southeast direction of the tanks within the farm and the anticipated principal direction of the groundwater flow and transport for the WMA-C area at closure.

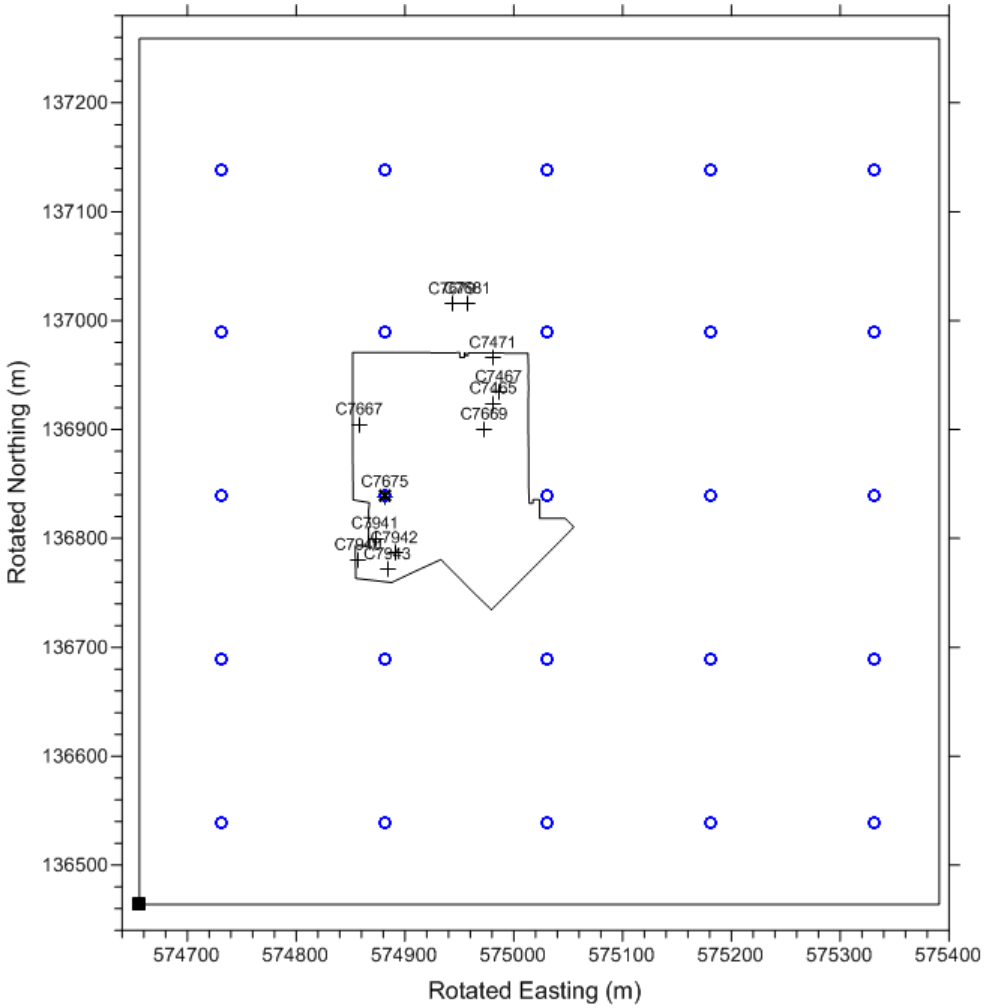

Figure 12. Locations of the direct push boreholes (black crosses) and the pseudo-wells (blue circles).

Multiple realizations of lithofacies distribution were generated using sequential indicator simulation (SISIM) method, onto the modeling domain. SISIM transforms the categorical lithofacies into a vector of indicator data, and defines a random path through the domain, constrained so that each grid node is only

visited once. During the simulation of the lithofacies at each grid node, the conditional probability of occurrence of each lithofacies is established using simple or ordinary kriging with the conditioning information of nearby original indicator data as well as previously simulated indicator values, upon which a cumulative distribution function is defined by adding the corresponding probabilities of occurrences of all lithofacies categories. With a randomly drawn probability value, a simulated value of the lithofacies is then assigned based on the cumulative distribution function (Goovaerts 1997, Deutsch and Journel 1998).

The geostatistical modeling domain for this study was defined with a horizontal resolution of 5 m by 5 m, and vertical resolution of 1 m. There are 148 x 160 x 116 (~ 2.75 million) grid nodes (Figure 13) in the 3-D domain. Considering the data coverage along the boreholes, the simulated lithofacies 1, 2, and 3 were kept only for those grids falling within H1, H2-Fine and H2-Coarse. The rest of the grids were replaced with the modeled layers generated by WRPS in (RPP-RPT-56356) as insufficient conditioning data were not available below the H2-silt unit.

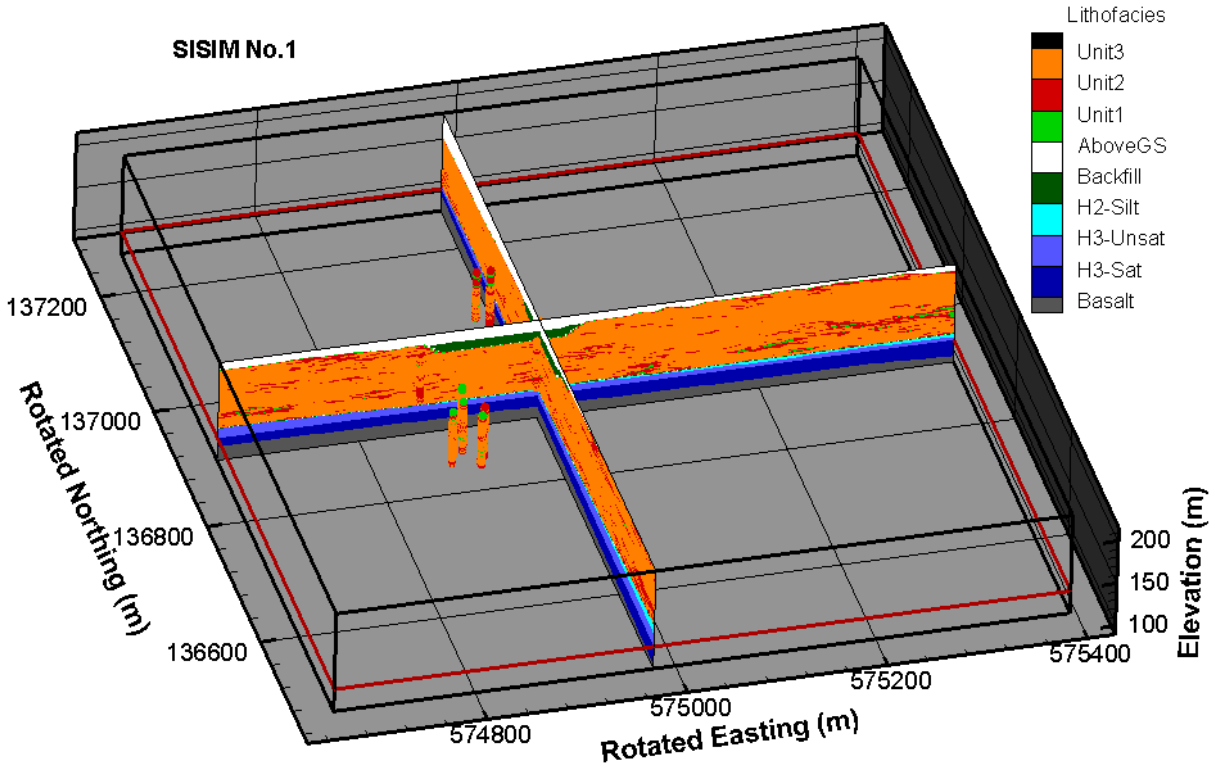

Figure 13. An example realization of lithofacies generated using SISIM. The two transects are at Rotated Easting of 574975 m and Rotated Northing of 136900 m. The red boundary indicates the water table level at the elevation of 121 m.

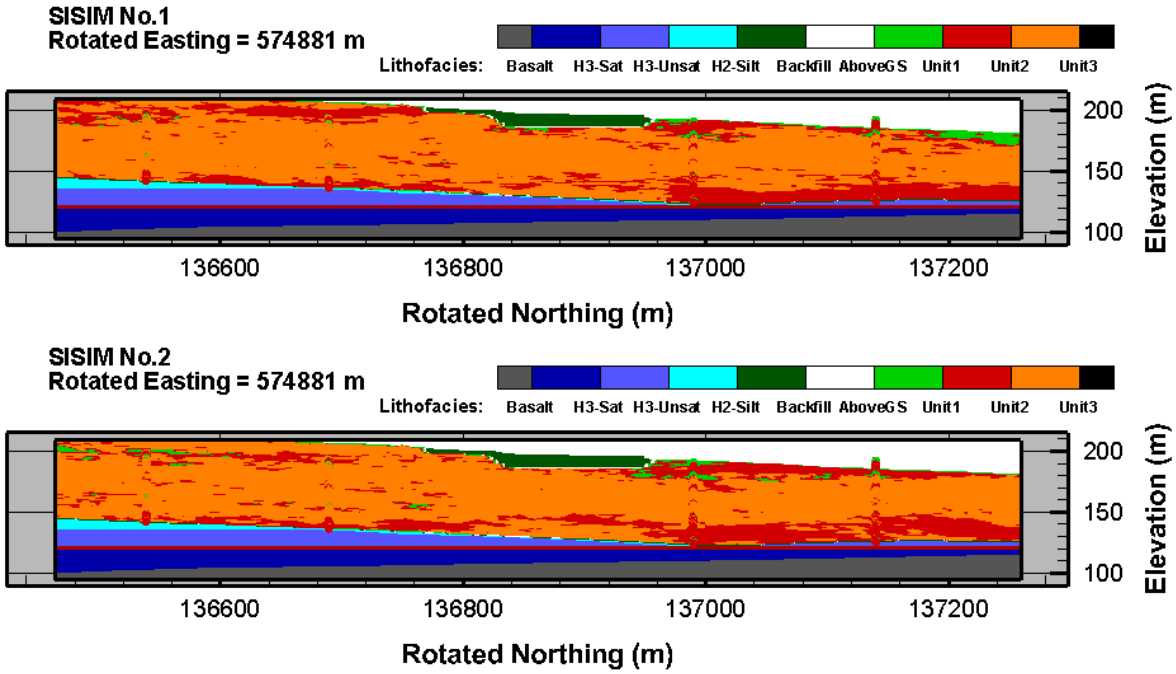

Figure 14. Transacts of two example realizations of lithofacies generated using SISIM.

Figure 14 shows transacts of two example realizations of lithofacies (Unit1/2/3) generated using SISIM, from base of backfill (where present) to base of H2 Coarse. Information regarding H2 Silt, H3, and Basalt was generated from unit surfaces developed by WRPS in (RPP-RPT-56356).

As shown in Figure 13 and Figure 14, each of the realizations honors borehole data and variogram models, such as spatial continuity and correlation patterns and dip angle. In the simulated lithofacies, one can see increased gravel lithofacies (unit 2) in the upper and lower portions of unsaturated Hanford strata, which correspond to H1 and H2 coarse unit strata. Therefore, these realizations will allow assessment of the impact of heterogeneous distribution of gravel and sand within H1 and H2 strata for comparison with model results that assume homogeneous properties within each stratigraphic layer.

6.0 Summary

In this study, KUT data derived from spectral gamma radiation logging performed at selected boreholes at the WMA-C was used to identify lithofacies and generate multiple realizations of lithofacies distributions were generated. This analysis provides an alternative conceptual model for the subsurface geology beneath WMA C that considers the detailed heterogeneity of sediments within the major hydrogeologic units. This alternative conceptual model provides the basis for a quantitative modeling analysis being performed at PNNL under separate funding using the ASCEM (Advanced Simulation Capability for Environmental Management) Toolset, which will be used to perform an initial evaluation of the impacts of heterogeneities on past leaks and tank residuals at the WMA C.

Further work in the geostatistical lithofacies identification and simulation study may include the following:

- Evaluation of whether the lateral extent of the grid is sufficient after testing of flow and transport simulations with 100 realizations of the geostatistical lithofacies model.
- Generation of other alternative conceptual models where modification of horizontal: vertical anisotropy ratio is considered
- Examination of other alternative lithofacies identification using combined KUT and moisture content data, e.g., data shows high moisture tail that may help define an additional lithofacies

7.0 References

Banfield, J. D. and A. E. Raftery (1993). "Model-based Gaussian and non-Gaussian clustering." Biometrics: 803-821.

Bierkens, M. F. (1996). "Modeling hydraulic conductivity of a complex confining layer at various spatial scales." Water Resources Research **32**(8): 2369-2382.

Deutsch, C. V. (2002). Geostatistical Reservoir Modeling. New York, Oxford University Press.

Deutsch, C. V. (2006). "A sequential indicator simulation program for categorical variables with point and block data: BlockSIS." Computers & Geosciences **32**(10): 1669-1681.

Deutsch, C. V. and A. G. Journel (1998). "GSLib." Geostatistical software library and user's guide: 369.

Ecology, et al. (1989). "Hanford Federal Facility Agreement and Consent Order." Washington State Dept. of Ecology, US Environmental Protection Agency, and the US Department of Energy.

Fraley, C. and A. E. Raftery (2002). "Model-based clustering, discriminant analysis, and density estimation." Journal of the American Statistical Association **97**(458): 611-631.

Freedman, V. L., et al. (2014). "A high-performance workflow system for subsurface simulation." Environmental Modelling & Software **55**: 176-189.

Freshley, M., et al. (2012). Advanced Simulation Capability for Environmental Management (ASCEM) Phase II Demonstration, USDOE Office of Environmental Management (EM)(United States); Los Alamos National Laboratory (LANL), Los Alamos, NM (United States); Pacific Northwest National Laboratory (PNNL), Richland, WA (United States); Lawrence Berkeley National Laboratory (LBNL), Berkeley, CA (United States);; Savannah River Site (SRS), Aiken, SC (United States).

Galford, J. E., et al. (2009). Field Test Results of a New Neutron Induced Gamma Ray Spectroscopy Geochemical Logging Tool. SPE Annual Technical Conference and Exhibition, Society of Petroleum Engineers.

Goovaerts, P. (1997). "Geostatistics for Natural Resources Evaluation." Oxford University Press.

Hertzog, R., et al. (1989). "Geochemical logging with spectrometry tools." SPE Formation Evaluation **4**(02): 153-162.

Kumar, A. and G. R. Kear (2003). "Lithofacies classification based on spectral yields and borehole microresistivity images."

Lau, J. W. and P. J. Green (2007). "Bayesian model-based clustering procedures." Journal of Computational and Graphical Statistics **16**(3): 526-558.

Maiti, S., et al. (2007). "Neural network modelling and classification of lithofacies using well log data: a case study from KTB borehole site." Geophysical Journal International **169**(2): 733-746.

Ritzi, R. W. (2000). "Behavior of indicator variograms and transition probabilities in relation to the variance in lengths of hydrofacies." Water Resources Research **36**(11): 3375-3381.

Rubin, Y. and A. G. Journel (1991). "Simulation of non-Gaussian space random functions for modeling transport in groundwater." Water Resources Research **27**(7): 1711-1721.

Scheibe, T. D., et al. (2006). "Transport and biogeochemical reaction of metals in a physically and chemically heterogeneous aquifer." Geosphere **2**(4): 220-235.

Schwarz, G. E. (1978). "Estimating the dimension of a model." Annals of Statistics **6**(2): 461-464.

White, M. D. and M. Oostrom (2006) STOMP Subsurface Transport Over Multiple Phases, Version 4.0, User's Guide. PNNL-15782.

Yabusaki, S. B., et al. (2011). "Variably saturated flow and multicomponent biogeochemical reactive transport modeling of a uranium bioremediation field experiment." Journal of Contaminant Hydrology **126**(3-4): 271-290.

Distribution

No. of Copies

1 **External Distribution**

Washington River Protection Solutions

Marcel Bergeron (PDF)

6 **Local Distribution**

Pacific Northwest National Laboratory

Yi-Ju Bott (PDF)

Mike Fayer (PDF)

Vicky Freedman (PDF)

Z. Jason Hou (PDF)

Chris Murray (PDF)

Information Release (PDF)

Pacific Northwest
NATIONAL LABORATORY

Proudly Operated by **Battelle** *Since 1965*

U.S. DEPARTMENT OF
ENERGY

902 Battelle Boulevard
P.O. Box 999
Richland, WA 99352
1-888-375-PNNL (7665)

www.pnnl.gov